

Limnol. Oceanogr., 46(8), 2001, 2073–2080
 © 2001, by the American Society of Limnology and Oceanography, Inc.

An in situ instrument for planar O₂ optode measurements at benthic interfaces

Abstract—A new in situ instrument for two-dimensional mapping of oxygen in coastal sediments is presented. The measuring principle is described, and potential mechanical disturbances, solute and particle smearing associated with the measurements, and calibration routines are evaluated. The first in situ measurements obtained in two different benthic communities are presented. In a shallow photosynthetic sediment (1 m of water depth), an extensive horizontal and temporal variation in the O₂ distribution caused by benthic photosynthesis and irrigating fauna was resolved. Repetitive planar optode measurements performed along a transect in central Øresund, Denmark (17 m of water depth) revealed a positive correlation between the apparent O₂ penetration depths (OP) measured with a lateral distance <5.0 mm, whereas OP measured with a larger horizontal distance (up to 50 m) were not correlated. Consequently, the OP varied in patches with a characteristic size of 5.0 mm. The instrument described is a powerful new tool for in situ characterization of spatiotemporal variations in O₂ distributions within benthic communities. The

instrument can be adapted for use at full ocean depths, e.g., on deep-sea landers or remote operating vehicles.

Distribution and exchange of O₂ are key measures for investigating benthic communities. Traditionally, benthic O₂ dynamics are either determined from concentration changes within sediment enclosures—i.e., benthic chambers—or from O₂ microsensor profiles (e.g., Rasmussen and Jørgensen 1992; Glud et al. 1994a). Total exchange measurements that use benthic flux chambers integrate effects of sediment heterogeneity and irrigation, whereas microsensor techniques allow detailed measurements of oxygen concentration profiles and dynamics but only at a limited number of points. However, the recent introduction of planar O₂ optodes to aquatic biology (Glud et al. 1996) now allows two-dimensional quantification of the spatiotemporal variations

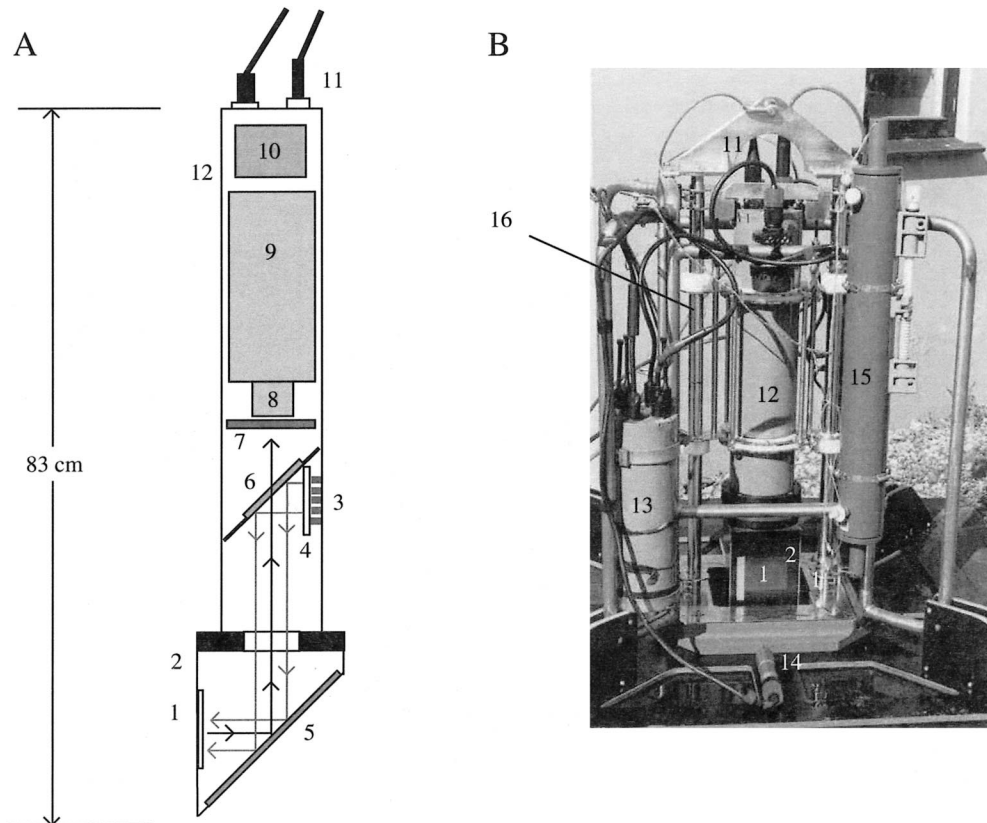


Fig. 1. (A) Illustration of the central housing and the periscope head. (B) A photograph of the complete instrument just prior to deployment. (1) Planar optode, (2) sensor window, (3) LEDs, (4) diffuser, (5) mirror, (6) dichroic mirror, (7) excitation filter, (8) lens, (9) CCD camera, (10) electronics controlling the excitation light, (11) connectors (one optic and one electric), (12) central housing, (13) battery for video and light, (14) video camera, (15) Niskin bottle, and (16) positioning elevator. See text for more explanation.

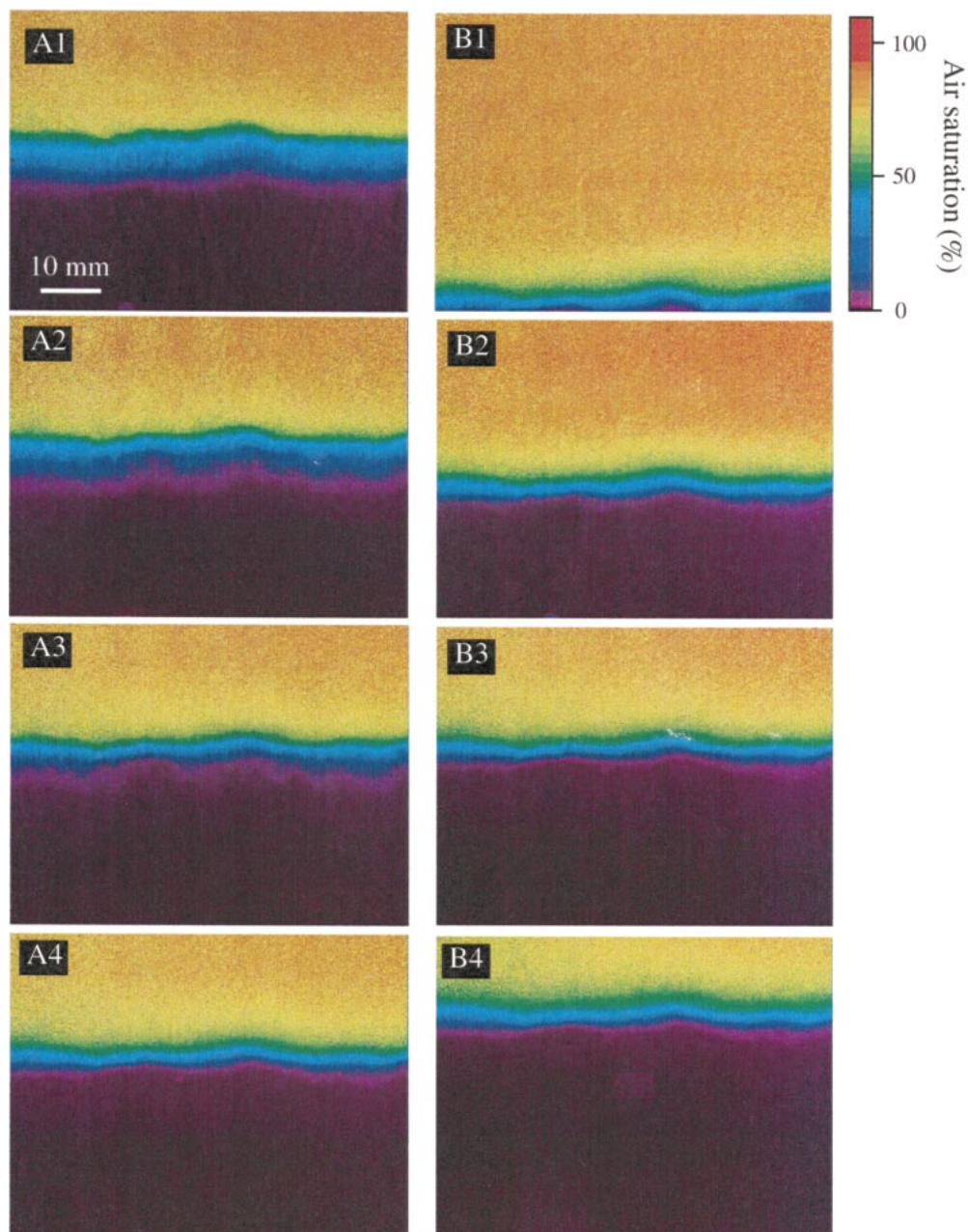


Fig. 2. (A) Series of O_2 images recorded after insertion of the sensor-equipped periscope head. The individual images were acquired after 2, 75, 310, and 490 s, respectively (listed from the top). (B) Series of O_2 images recorded after 600 s with the sensor equipped periscope head at four different vertical positions. A scale bar that expresses the air saturation as a color code is included.

in O_2 distribution at heterogeneous benthic interfaces with a spatial resolution of <0.1 mm over areas of several cm^2 .

The measuring principle for O_2 optodes is based on the dynamic quenching (Kautsky 1939) of a fluorescent indicator by oxygen. In the absence of O_2 , the fluorophore absorbs light and emits the absorbed energy as fluorescence with a defined intensity and lifetime. In the presence of O_2 , quenching decreases both fluorescent intensity and lifetime (Klimant et al. 1995; Hartmann and Ziegler 1996). For planar sensing, the fluorescent indicator is immobilized on thin

transparent foils, and the O_2 -sensitive fluorescence intensity or lifetime distribution on the foil is quantified by a digital camera system (Glud et al. 1996; Holst et al. 1998). The use of planar optodes partly overcomes the limitations of describing oxygen distribution at heterogeneous three-dimensional interfaces with one-dimensional microprofiles (Glud et al. 2000; Kühl and Revsbech 2001). Benthic O_2 images have revealed hot spots and O_2 microniches that are either overlooked or ignored with existing techniques (Glud et al. 1998, 1999; Fenchel and Glud 2000; König, Glud, and Kühl

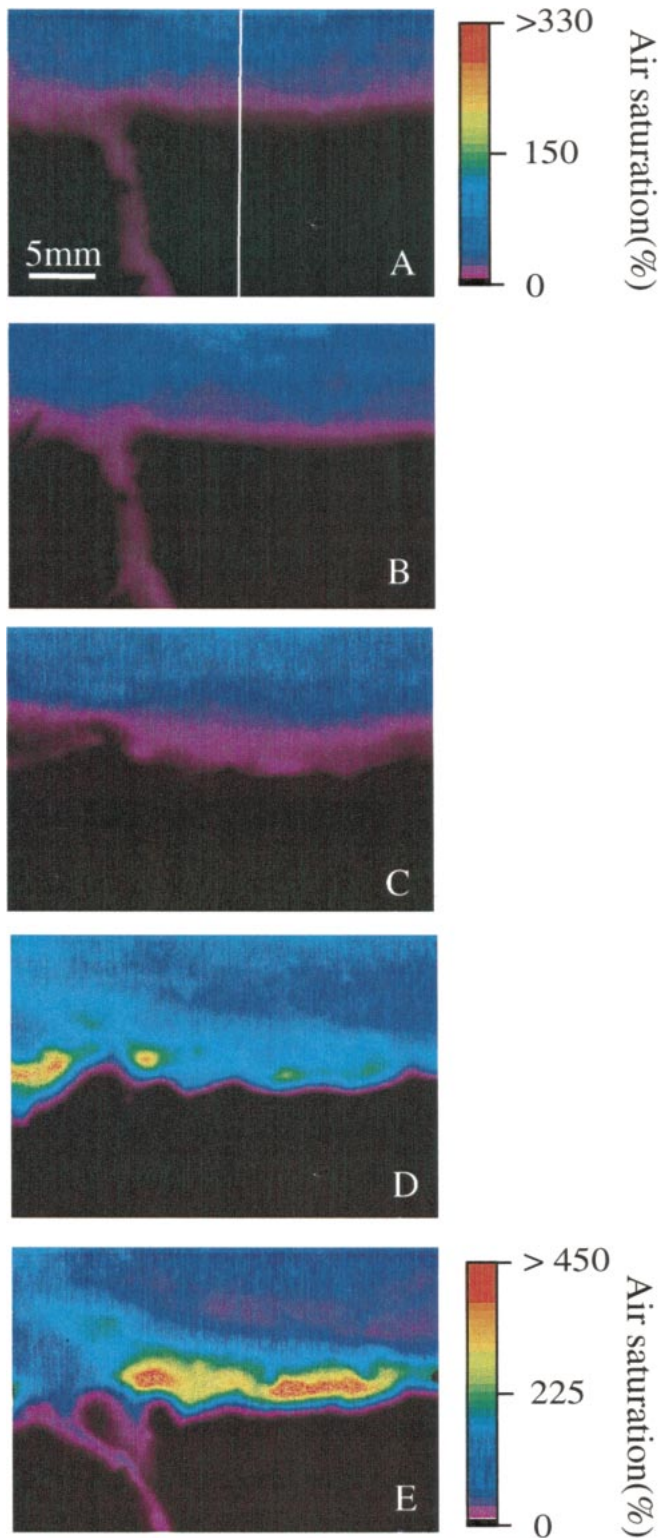


Fig. 3. Oxygen distribution in a shallow photosynthetic sediment at 1 m depth. A series of O_2 images recorded in situ at 1 h intervals after insertion of the sensor equipped periscope head. The images were obtained at 7:33, 8:33, 9:33, 10:33 and 11:33 h, at which time the down-welling irradiance at the air-water interface equaled 1, 8, 240, 633, and 1,102 $\mu\text{mol photons m}^{-2} \text{s}^{-1}$. The air saturation for the first four images is expressed on the upper scale bar, and the lower scale bar belongs to image (E). The white line in (A) represents the row of pixels presented in Fig. 4.

unpubl.). So far, all planar optode measurements have been conducted in the laboratory on recovered or manipulated samples.

In order to minimize recovery artifacts and mechanical disturbances, self-operating vehicles for deploying benthic chambers and O_2 microsensors have been constructed over the past few decades (for reviews, see Tengberg et al. 1995; Reimers and Glud 2000). Here we present a new benthic instrument capable of obtaining online in situ images of the two-dimensional benthic O_2 distribution in sediments of shallow water (<25 m, limited by cable length). In situ planar optode measurements from two coastal sites are presented and discussed.

Instrument description—The design of the instrument was inspired by previously described inverted periscopes developed for documenting sediment characteristics and fauna occurrence in surface sediments (Rhoads and Germano 1982; Nilsson and Rosenberg 2000). The central instrument housing was mounted on an inverted periscope and contained the excitation light source, optical filters, an electrically cooled Charge Coupled Device (CCD) camera (SensiCam, PCO Computer Optics) and associated electronics (Fig. 1A). The fast-gate-able 12-bit CCD camera was connected via a fiber-optical link to a personal computer (PC) at the surface. By use of a modulated CCD camera in combination with a fast-responding excitation source, both the fluorescent lifetime and intensity of the sensor foil could be used as the O_2 sensitive parameter.

In order to ensure precise timing of the excitation light and the image acquisition, the PC was connected to a pulse delay generator (DG535, SRS Stanford Research Systems). More details on the camera and the associated software are given elsewhere (Holst et al. 1998). An array of 5×5 blue light-emitting diodes (LED) ($\lambda = 470 \text{ nm}$ HLMP-CB15, DCL Components) (Fig. 1A) was used as the excitation light source. The excitation light passed a diffuser and was reflected via a dichroic mirror (Danish Electronics, Light & Acoustics) toward the periscope head, where a second mirror reflected it toward the sensor window. The red fluorescent light of the planar optode followed the same path in the opposite direction but passed the dichroic mirror and a long-pass filter (OG 570, Schott) before entering the CCD camera (Fig. 1A). Images of the fluorescence were acquired as 12-bit TIFF-format images for later calibration (see below). The image acquisition was controlled online via a custom-made, 30 m underwater cable (MacArtney) that contained both fiber-optic and coaxial connections between instrument and the PC.

The frame of the periscope head was made of 1 mm titanium. A 50-mm-thick cast Plexiglas cone, sealed between the central housing and the periscope head ensured light passage between the two compartments. The hollow periscope head contained a mirror fixed to the angled wall and was sealed with the replaceable sensor window (Fig. 1A). Prior to deployment, the periscope head was filled with degassed, distilled water through two Tygon tubings. During deployment, the flexible tubings acted as pressure compensation by equalizing any hydrostatic pressure difference between the inside and outside of the periscope head. The use of de-

gassed water prevented the development of gas bubbles in the periscope head after a temperature increase. The planar optode was fixed to the sensor window by a thin layer of silicone grease, and the remaining part of the window was covered with black tape, to block ambient light.

The central housing of the instrument was fixed in an elevator allowing vertical adjustment of the sensor window in increments of 1.0 mm (KC-Denmark) (Fig. 1). The movement was imposed by a 24 V DC motor placed in a pressure-compensated cast Plexiglas housing (not visible in Fig. 1). The motor, and thereby the position, of the central housing, was controlled from the surface via the cable. The central housing had a total migration length of 25 cm, defined by the distance between two switches that were activated by neodymium magnets mounted on one of the steering rods of the elevator. The motor thus stopped when the central housing reached the end points. All power required by the instrument was supplied via the cable from the ship.

Instrument deployment—For in situ deployments, the instrument was mounted on a tripod frame, which was lowered slowly by a wire from the ship (or from the pier). After reaching the sea floor, a stabilization period of at least 30 min was allowed prior to any measurements. Temperature, salinity, and flow velocity of the bottom water were recorded by a Recording Current Meter (RCM9, Aanderaa Instruments) mounted on the instrument frame. Additionally, a video camera (MicroSeaCam, Deep Sea Power and Light) connected to a TV screen allowed visual inspection of the measuring site, whereby the position of the planar optode relative to the sediment surface could be estimated. Prior to insertion of the periscope head, a series of images (series 1) were recorded in the bottom water. Subsequently the central housing was lowered at a speed of 1 mm s⁻¹ until approximately half the sensor was covered by sediment. Visual inspection showed no disturbance of the sediment surface structure during insertion (otherwise the deployment was abandoned). After recording a series of images at the sediment water interface (series 2), the central housing was lowered by an additional 10 cm, and a third series of images were recorded with the complete sensor foil in the anoxic sediment (series 3). Finally, prior to instrument recovery, a Niskin bottle fixed to the frame was released via the moving elevator. A subsample of the collected water was used for determination of the bottom water O₂ concentration by Winkler titration.

Planar optodes—For the present study, we used planar O₂ optodes based on the fluorophore, ruthenium (III)-Tris-4,7-diphenyl-1,10-phenanthroline [Ru(diph)₂] embedded in plasticized PVC (O-nitrophenyloctylether). The sensing layer was prepared by dissolving 10 mg fluorophore, 500 mg PVC and 500 mg plasticizer in 10 ml THF. The mixture was immobilized on a transparent polyester support foil (Mylar, Dupont) by a knife-coating procedure. The indicator concentration in the cured sensing layer was 2% (w/w). In order to avoid interference from scattering particles in the sediments, the cured sensing layer was covered by an optically insulating black layer of Teflon that consisted of 0.5 g Teflon AF 1,600 dissolved in 10 g perfluorodecalin and 0.5 g fine

graphite particles. The three layered planar optodes had a total thickness of ~250 μm, made of the 175-μm-thick support foil, the 10-μm-thick layer of immobilized fluorophore, and the 50–70-μm-thick layer of optical insulation.

Calibration and calculations—The TIFF images obtained were calibrated against O₂ by use of a modified Stern-Volmer equation (Glud et al. 1996; Holst et al. 1998):

$$\frac{I}{I_0} = \frac{\tau}{\tau_0} = \alpha + \frac{1}{(1 + K_{sv}C)}(1 - \alpha) \quad (1)$$

where I_0 and I are the fluorescent intensities at anoxia and in the presence of O₂ at a concentration C , respectively, and τ_0 and τ are the equivalent fluorescent lifetimes. α is the fraction of nonquenchable signal and K_{sv} the quenching coefficient. With use of the images obtained in the bottom water and in the anoxic sediment, I_0 , α , and K_{sv} for all 640 × 480 pixels of the acquired images were calculated and used for the subsequent calibration. In the following, calibrated images are referred to as O₂ images. The camera system allowed the O₂ distribution to be quantified either by the fluorescent light intensity or the fluorescent lifetime. All data in this study were obtained by the so-called “shark-fin” approach for quantification of the fluorescent lifetime. By use of this technique, the ratio between the excited and nonexcited sensor signal is calculated during well-defined pulsing of the excitation light (Hartman et al. 1997). A more detailed discussion of various approaches for quantifying fluorescent lifetime is given elsewhere (Holst et al. 1998; Glud et al. 2000).

Laboratory tests—Prior to in situ deployments a series of test measurements were performed in the laboratory. Homogenized sediment (~400 kg) was recovered from the harbor of Helsingør and placed in aquaria. The sediment was left for a 3-week period while the 10-cm-deep water column above the sediment was continuously renewed with fresh aerated seawater. The homogenized reestablished sediment had a porosity of 0.69 ± 0.04 ($n = 12$) and an organic carbon content of 0.7% ± 0.2% ($n = 12$). For the laboratory measurements, the camera was equipped with a macro lens (Tevidon, F1.4/25 mm) that imaged an area of 66.0 × 49.5 mm. Given the size of the camera chip (640 × 480), this resulted in a spatial image resolution of 103 × 103 μm per pixel.

The response time of a planar optode depends on the time it takes for O₂ dissolved in the optical insulation and the sensing layer to achieve thermodynamic equilibrium with the surrounding medium. Because of the relatively thick optical insulation applied in this study, a steady-state signal was obtained after ~300–400 s (Fig. 2A). Therefore, in subsequent measurements, we acquired a series of images until steady state was observed and used the last images for further analysis. The measuring approach requires that an optode previously exposed to O₂-rich bottom water is subsequently inserted into anoxic sediment strata. It must be noted that O₂ dissolved in the sensor materials can affect the redox condition at the oxic-anoxic interface. It is therefore recommended to use optodes with as thin an optical insulation or for nonscattering environments potentially transparent op-

todes without optical insulation (Holst and Grunwald 2001). Planar optodes with a thinner optical insulation than applied here can, however, be easily constructed (Glud et al. 1996). Thinning of the optical insulation also lowers the response time of the sensors to a few seconds, which would be required for studies on irrigation patterns or gross photosynthesis (Glud et al. 1996, 1999; Klimant et al. 1997).

In order to investigate the extent that periscope insertion resulted in smearing of the O₂ signal, the periscope was lowered stepwise into the sediment, and a time series of images was acquired at each depth. It was demonstrated that the O₂ penetration depth and microtopographic structures remained unaffected by subsequent lowering of the periscope head (Fig. 2B). Thus, oxidation imposed by sensor insertion and disturbance of surface microtopography was negligible in this particular setup. These observations can, however, not be generalized, and further investigations in various sediments are required to evaluate the potential effects. It is well known that insertion of coreliners, sediment chambers, or sediment cameras introduce a vertical particle smearing (e.g., Nilsson and Rosenberg, 2000). By depositing fluorescent particles at the sediment surface and subsequent insertion of the periscope head (without any optical insulation), such an effect was also demonstrated for our instrument (data not shown). This unavoidable particle smearing can potentially affect the O₂ distribution within the sediment. However, for the silty sediment used in our laboratory test, the effect was of minor importance (Fig. 2B). The importance of smearing effects will be sediment dependent, and it is clear that mechanical forcing that involves larger obstacles (shell fragments, etc.) will introduce major disturbance of the surface sediment structure and, thereby, the O₂ distribution. Future experience will elucidate the extent of this potential problem for various sediment types. As for all instruments designed for quantification of benthic exchange rates, the placement of the instrument at sediment surface will change the local hydrodynamics. To what extent this affect the O₂ distribution at the measuring site depends on the sediment permeability and the impedance imposed by the diffusive boundary layer (DBL) (Glud et al. 1994b, 1995; Jørgensen 2001) and has, as always, to be evaluated for each given site.

In situ measurements in a shallow water photosynthetic community—The instrument was deployed in 1m of water in the harbor of Helsingør (December 2000). Patches of cyanobacteria, diatoms, and colorless sulfur bacteria covered the silty sediment surface. The macrofauna was dominated by small specimens of *Nereis diversicolor*. The temperature was 5°C, the salinity 26‰, the O₂ content of the water close to air saturation (95%–110%) during the diel cycle, and the free flow velocity low (<1 cm s⁻¹) and from varied directions. The downwelling irradiance (measured by a LI-Cor LI-192SA irradiance sensor) reached a maximum of 1,102 μmol photons m⁻² s⁻¹ around noon. In that experiment, a spacer ring was placed between the camera and the lens, and the images consequently covered an area of 32 × 24 mm at a spatial resolution of 50 × 50 μm per pixel. Images were recorded at a 1-h interval, and Fig. 3 presents data obtained during the morning. The images reflect an extensive horizontal variation in the O₂ distribution, including a periodi-

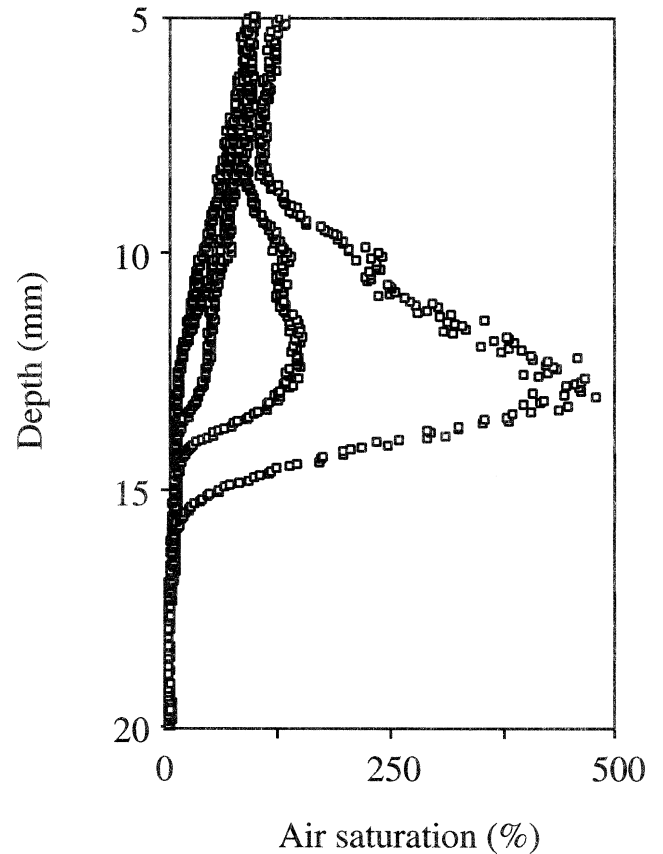


Fig. 4. Concentration profiles extracted from the O₂ images presented in Fig. 3. The gradual increase in the air-saturation with increasing irradiance is apparent.

cally irrigated burrow apparent in Fig. 3A,B,E. Occasionally, the burrow became anoxic and appeared to be reconstructed in the last of the images. As the irradiance increased, patches supporting benthic photosynthesis appeared; however, the active areas (Fig. 3D) could be disturbed, where the sediment surface appeared to have been restructured along with the burrow (Fig. 3E). The O₂ concentration of the overlying water increased with the photosynthetic activity, and the extension of the oxic zone increased during the day. Supersaturated water packages were observed downstream from the active phototrophic community, the local flow scenario probably influenced by the periodically flushing of the neighboring burrow (Fig. 3). Occasionally, undersaturated water packages were also observed, probably after passing reduced sediment patches. It was not possible to resolve the exact position of the sediment surface by the external video camera (Fig. 1B). In future studies, high-resolution sediment images from outside the periscope head and the use of defined pinholes in the planar optodes will allow O₂ images and sediment images to be aligned. Thereby, the position of the sediment surface in relation to the O₂ distribution can be established. The use of transparent optodes can also be an option in some cases (Holst and Grunwald in press).

Each O₂ image contains 640 vertical O₂ microprofiles, and examples extracted from the images are presented (Fig. 4). Because the relative position of the sediment surface was

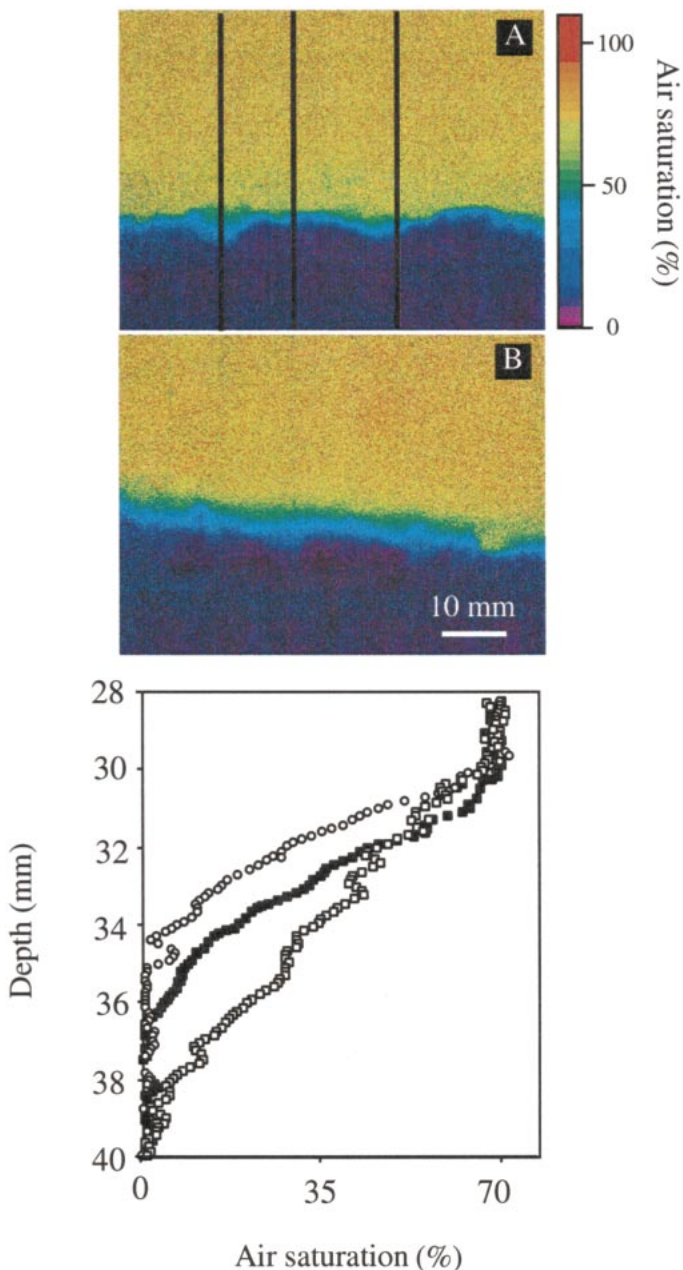


Fig. 5. Oxygen distribution in coastal sediment at 17 m water depth. Two O₂ images recorded with an approximate lateral distance of 70 m. Three rows of pixels (indicated in A) were extracted and presented as traditional O₂ concentration profiles in the lower panel. A scale bar that expresses the air saturation as a color code is included.

poorly defined it was not possible to separate the O₂ gradients into two sections related to DBL and the sediment, respectively. However, the O₂ images in principle allow for the determination of, the diffusive exchange rates, the net photosynthesis and the respiration, as shown in previous studies (Glud et al. 1999; Fenchel and Glud 2000).

In situ measurements in a coastal sediment—The instrument was also deployed at a 17-m-deep site in central Øre-

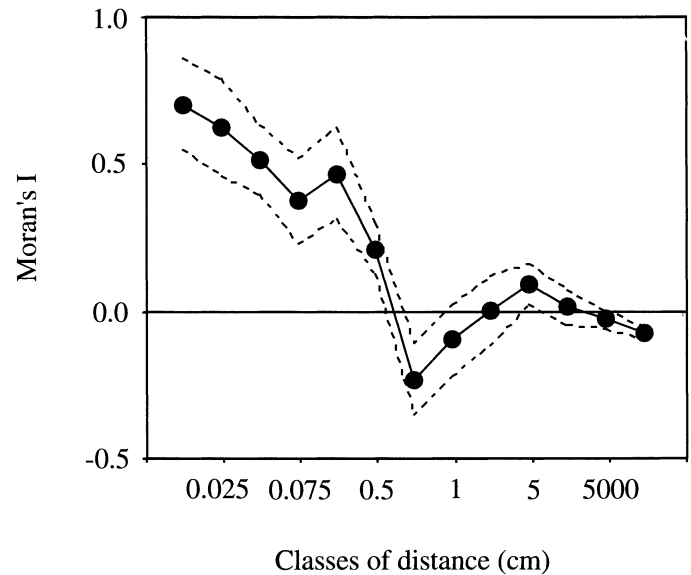


Fig. 6. Moran's *I* autocorrelation coefficient as a function of classes of distance of the apparent O₂ penetration depth. Broken lines indicate the 95% confidence interval.

sund, Denmark. The in situ temperature was 9°C, the salinity 33.9‰, the bottom water 70% saturated (202 μM), and the free flow velocity around 10 cm s⁻¹. Because a relatively deep O₂ penetration depth was expected, the spacer between camera and lens was removed, and the spatial resolution was consequently lowered to the original 103 × 103 μm per pixel. Eight repetitive deployments were performed with a lateral distance of ~10 m between each deployment. The first and last of the obtained O₂ images are presented (Fig. 5). The penetration depth of oxygen is closely related to the O₂ consumption rate and thereby the benthic mineralization rate (e.g., Bouldin 1968). At the investigated site the apparent O₂ penetration depth (OP) varied between 4.2 and 13.3 mm, with an average value for the 5,120 O₂ microprofiles of 8.07 ± 2.19 mm. In order to evaluate the horizontal scale on which the O₂ consumption varied, 34 O₂ microprofiles were extracted from each O₂ image. The spatial autocorrelation estimated as Moran *I* coefficients (Moran 1950; Legendre and Legendre 1998) was calculated from the following 13 classes of distance between individual profiles: 0–0.015, 0.015–0.025, 0.025–0.05, 0.05–0.075, 0.075–0.125, 0.125–0.5, 0.5–0.75, 0.75–1, 1–2, 2–5, 5–1,000, 1,000–5,000, and 5,000–7,000 cm. Moran's *I* and Pearson's correlation coefficients are closely related, and positive and negative values indicate positive and negative autocorrelation, respectively. The spatial autocorrelation coefficients estimated as Moran's *I* were tested for significance according to Legendre and Legendre (1998). Plotted in a spatial correlogram (Cliff and Ord 1981), the change of sign appeared to be between the distance class from 0.125–0.5 to 0.5–0.75 cm (Fig. 6). This shows that the OP varied in patches of a lateral distance of <5.0 mm at the investigated site. The data for the first time allow spatial scales for the variability in O₂ penetration depths (i.e., mineralization activity) to be evaluated. However, it has to be emphasized that we have only included images that were not visually affected by macro-

fauna and therefore only represents seafloor areas where diffusion is the main transport mode.

Summary and future developments—The new instrument presented in this study allows in situ visualization of the oxygen dynamics at heterogeneous benthic interfaces at an unprecedented resolution. Effects of surface topography, sediment structure, and bioturbation on the oxygen distribution in sediments can be monitored at high spatiotemporal resolution. The next challenges are to optimize sensor materials and instrument settings for combined mapping of oxygen and sediment structure. Furthermore, planar sensors for other relevant biogeochemical variables like pH and CO₂ will be implemented. The present in situ instrument was designed for deployment in shallow waters and for online operation via cable connection to the surface. However, the central parts of the instrument, such as the electronics casing and periscope materials, have been designed to withstand full ocean depths of up to 6 km. For deep-sea application, an instrument module is now being designed that will have the capacity to operate autonomously for extended time periods on a deep-sea lander or as a module on a remote-operating vehicle.

Ronnie N. Glud

Marine Biological Laboratory
Copenhagen University
Strandpromenaden 5
DK-3000 Helsingør, Denmark

Anders Tengberg

Department of Analytical and Marine Chemistry
Göteborg University
S-41296 Göteborg, Sweden

Michael Kühn

Marine Biological Laboratory
Copenhagen University
Strandpromenaden 5
DK-3000 Helsingør, Denmark

Per O. J. Hall

Department of Analytical and Marine Chemistry
Göteborg University
S-41296 Göteborg, Sweden

Ingo Klimant

Institute of Analytical Chemistry, Micro- and Radiochemistry
Technical University of Graz
Stremayrgasse 16
A-8010 Graz, Austria

Acknowledgments

We acknowledge the support of the Carlsberg Foundation (R.N.G.), the Danish Natural Science Research Council (M.K.), The Swedish Research Council for Engineering Sciences (A.T. and P.O.J.H.), and the Max Planck Society (G.H.). Benly and Brian are thanked for their assistance and skillful maneuvering of R.V. *Ophelia*. H. Millqvist is thanked for technical assistance during instrument construction, and S. E. Larsen is acknowledged for his help with the statistical analysis. Two anonymous reviewers are thanked for constructive criticism that helped improve the manuscript.

Gerhard Holst

Max Planck Institute for Marine Microbiology
Celsiusstrasse 1
D-28359 Bremen, Germany

References

- BOULDIN, D. R. 1968. Models for describing the diffusion of oxygen and other mobile constituents across the mud-water interface. *J. Ecol.* **56**: 77–87.
- CLIFF, A. D., AND J. K. ORD. 1981. Spatial processes: Models and applications. Pion Limited.
- FENCHEL, T., AND R. N. GLUD. 2000. Benthic primary production and O₂-CO₂ dynamics in a shallow water sediment: Spatial and temporal heterogeneity. *Ophelia* **53**: 159–171.
- GLUD, R. N., J. K. GUNDERSEN, B. B. JØRGENSEN, N. P. REVSBECH, AND H. D. SCHULZ. 1994a. Diffusive and total oxygen uptake of deep-sea sediments in the eastern South Atlantic Ocean: In situ and laboratory measurements. *Deep-Sea Res.* **41**: 1767–1788.
- , AND N. B. RAMSING. 2000. Electrochemical and optical oxygen microsensors for in situ measurements, p. 19–73. *In* J. Buffle and G. Horvai [eds.], In situ analytical techniques for water and sediment. John Wiley & Sons.
- , ———, N. P. REVSBECH, AND B. B. JØRGENSEN. 1994b. Effects on the benthic diffusive boundary layer imposed by microelectrodes. *Limnol. Oceanogr.* **39**: 462–467.
- , ———, ———, AND M. HÜTTEL. 1995. Calibration and performance of the stirred flux chamber from the benthic lander Elinor. *Deep-Sea Res.* **42**: 1029–1042.
- , M. KÜHL, O. KOHLS, AND N. B. RAMSING. 1999. Heterogeneity of oxygen production and consumption in a photosynthetic microbial mat as studied by planar optodes. *J. Phycol.* **35**: 270–279.
- , N. B. RAMSING, J. K. GUNDERSEN, AND I. KLIMANT. 1996. Planar optodes, a new tool for fine scale measurements of two-dimensional O₂ distribution in benthic communities. *Mar. Ecol. Prog. Ser.* **140**: 217–226.
- , C. M. SANTEGOEDS, D. DE BEER, O. KOHLS, AND N. B. RAMSING. 1998. Oxygen dynamics at the base of a biofilm studied with planar optodes. *Aquat. Microb. Ecol.* **14**: 223–233.
- HARTMANN, P., AND W. ZIGLER. 1996. Lifetime imaging of luminescent oxygen sensors based on all-solid state technology. *Anal. Chem.* **68**: 4512–4514.
- , G. HOLST, AND D. W. LÜBBERS. 1997. Oxygen flux fluorescence lifetime imaging. *Sensors Actuators B* **38–39**: 110–115.
- HOLST, G., AND B. GRUNWALD. 2001. Luminescence lifetime imaging with transparent oxygen optodes. *Sensors Actuators B* **74**: 78–90.
- , O. KOHLS, I. KLIMANT, B. KÖNIG, M. KÜHL, AND T. RICHTER. 1998. A modular luminescence lifetime imaging system for mapping oxygen distribution in biological samples. *Sensors Actuators B* **51**: 163–170.
- JØRGENSEN, B. B. 2001. Life in the diffusive boundary layer, p. 348–367. *In* B. Boudreau and B. B. Jørgensen [eds.], The benthic boundary layer. Oxford Univ. Press.
- KAUTSKY, H. 1939. Quenching of luminescence by oxygen. *Trans. Faraday Soc.* **35**: 216–219.
- KLIMANT, I., V. MEYER, AND M. KÜHL. 1995. Fiber-optic oxygen microsensors, a new tool in aquatic biology. *Limnol. Oceanogr.* **40**: 1159–1165.
- , M. KÜHL, R. N. GLUD, AND G. HOLST. 1997. Optical measurements of oxygen and other environmental parameters in

- microscale: Strategies and biological applications. *Sensors Actuators B* **38–39**: 29–37.
- KÜHL, M., AND N. P. REVSBECH. 2001. Microsensors for the study of interfacial biogeochemical processes, p. 180–210. *In* B. Boudreau and B. B. Jørgensen [eds.], *The benthic boundary layer*. Oxford Univ. Press.
- LEGENDRE, P., AND L. LEGENDRE. 1998. *Developments in environmental ecology*, 20. Numerical ecology, 2nd English edition. Elsevier Science.
- MORAN, P. A. P. 1950. Notes on continuous stochastic phenomena. *Biometrika* **37**: 17–23.
- NILSSON, H. C., AND R. ROSENBERG. 2000. Succession in marine benthic habitats and fauna in response to oxygen deficiency: Analyzed by sediment profiling-imaging and grab samples. *Mar. Ecol. Prog. Ser.* **197**: 139–149.
- RASMUSSEN, H., AND B. B. JØRGENSEN. 1992. Microelectrode studies of seasonal oxygen uptake in a coastal sediment: Role of molecular diffusion. *Mar. Ecol. Prog. Ser.* **81**: 289–303.
- REIMERS, C., AND R. N. GLUD. 2000. In situ chemical sensor measurements at the sediment-water interface, p. 249–282. *In* M. Varney [ed.], *Chemical sensors in oceanography*. Gordon and Breach Science Publishers.
- RHOADS, D. C., AND J. D. GERMANO. 1982. Characterization of organism-sediment relations using sediment profile imaging: An efficient method of remote ecological monitoring of the seafloor (Remots™ systems). *Mar. Ecol. Prog. Ser.* **8**: 115–128.
- TENGBERG, A., AND OTHERS. 1995. Benthic chamber and profile landers in oceanography—a review of design, technical solutions and functioning. *Prog. Oceanogr.* **35**: 253–294.

Received: 2 April 2001

Amended: 23 August 2001

Accepted: 6 September 2001

Limnol. Oceanogr., 46(8), 2001, 2080–2087

© 2001, by the American Society of Limnology and Oceanography, Inc.

Measurement of local bed shear stress in streams using a Preston-static tube

Abstract—Local bed shear stress (τ_w) is a fluid dynamic parameter of importance in determining the physical and biological characteristics of stream-bed environments. Unfortunately, it is often difficult to measure τ_w under field conditions. Herein we describe the use of a Preston-static tube, which is essentially a surface-mounted Pitot-static tube, to measure τ_w in mountain streams. Our results indicate that it is possible to measure local shear stress quickly, consistently, and inexpensively in the field. This technique also provides high spatial resolution, which should allow for detailed in situ studies of local shear stress at scales relevant to lotic organisms. Such information will be invaluable in studies of benthic organisms and hydraulically relevant phenomena in the near-bottom zone of lotic systems.

There can be little doubt that near-bottom hydraulics, and shear stress (τ) in particular, remains one of the most important parameters for the study of bedload transport (e.g., Wilcock 1996; Blizard and Wohl 1998) and benthic ecology (e.g., Davis 1986; Carling 1992) in lotic environments. For example, one need only consider the Shield's curve, which predicts the movement of benthic sediments (e.g., Buffington and Montgomery 1997; Blizard and Wohl 1998), or examine the zonation of stream organisms (e.g., Robertson et al. 1997), to appreciate the importance of τ . This is because τ is partly a measure of the tractive (or frictional) forces per unit area of the bottom that results from the interaction of fluid moving past the bottom (i.e., the no-slip condition). The law of the wall, $u = (u_* / \kappa) \ln(z/z_0)$, where u is the mean streamwise velocity, u_* is the friction velocity given by $u_* = \sqrt{\tau/\rho}$, κ is the von Karman constant, z is the distance from the wall or boundary, and z_0 is the roughness height, can be used to determine u_* and thus τ (e.g., Nowell and Jumars 1984; White 1999). At the reach scale in lotic systems, the total shear stress, τ_0 , which includes the local bed

shear stress (or skin friction, τ_w) and the form (or pressure) drag of the various elements in the stream (e.g., bars, boulders, logs), can be determined from the depth-slope product, $\tau_0 = \rho g h S_o$, where g is the acceleration due to gravity, h is the average water depth in the reach, and S_o is the surface slope (see Buffington and Montgomery 1999; Manga and Kirchner 2000). It is the local shear stress, τ_w , however, that is a more appropriate parameter to measure at finer spatial scales corresponding to individual bed elements or biota. τ_w is the subject of this report.

Whereas τ_w is an essential hydraulic parameter to determine, there are a limited number of techniques that can be used to infer or to measure it (e.g., force balance methods, velocity profile methods, and mass transfer methods; Table 1; Winter 1977; Hanratty and Campbell 1983; Haritonidis 1989; Fernholz et al. 1996; Dade et al. 2001). For practical application under field conditions, these techniques fall into several categories, the most commonly used one of which uses vertical profiles or single or multiple measurements of velocity to estimate τ_w based on the law of the wall. Advances in instrumentation for the measurement of water velocity, including constant temperature anemometry (CTA), laser-Doppler (LDV), acoustic Doppler (ADV), and particle image velocimetry (PIV), have increased the spatial and temporal resolution at which velocity is measured, providing an opportunity to estimate τ_w and to compute Reynolds stresses from velocity fluctuations (e.g., Bouckaert and Davis 1998). Unfortunately, these techniques have limitations pertaining to their use under field conditions (e.g., CTA, LDV, and PIV; Hart et al. 1996; but see Tominaga and Nezu 1992, and Bertuccioli et al. 1999) and near boundaries (ADV; Finelli et al. 1999; Hoover and Ackerman pers. obs.), which are required in order to compute τ_w . Moreover, the relatively high instrumentation cost of CTA, LDV, and PIV, and the time and effort required in both categories, limits their application in most field conditions.